Analysis of the CDR3 length repertoire and the diversity of T cell receptor α and β chains in swine CD4+ and CD8+ T lymphocytes

CHUN-YAN WANG, YONG-XIANG FANG, GUO-HUA CHEN, HUAI-JIE JIA, SHUANG ZENG, XIAO-BING HE, YUAN FENG, SHOU-JIE LI, QI-WANG JIN, WEN-YU CHENG and ZHI-ZHONG JING

State Key Laboratory of Veterinary Etiological Biology, Key Laboratory of Veterinary Public Health of Ministry of Agriculture, Lanzhou Veterinary Research Institute, Chinese Academy of Agricultural Sciences, Lanzhou, Gansu 730046, P.R. China

Received January 10, 2016; Accepted February 20, 2017

DOI: 10.3892/mmr.2017.6601

Abstract. The T cell receptor (TCR) is a complex heterodimer that recognizes fragments of antigens as peptides and binds to major histocompatibility complex molecules. The TCR α and β chains possess three hypervariable regions termed complementarity determining regions (CDR1, 2 and 3). CDR3 is responsible for recognizing processed antigen peptides. Immunoscope spectratyping is a simple technique for analyzing CDR3 polymorphisms and sequence length diversity, in order to investigate T cell function and the pattern of TCR utilization. The present study employed this technique to analyze CDR3 polymorphisms and the sequence length diversity of TCR α and β chains in porcine CD4+ and CD8+ T cells. Polymerase chain reaction products of 19 TCR α variable regions (AV) and 20 TCR β variable regions (BV) gene families obtained from the CD4+ and CD8+ T cells revealed a clear band following separation by 1.5% agarose gel electrophoresis, and each family exhibited >8 bands following separation by 6% sequencing gel electrophoresis. CDR3 spectratyping of all identified TCR AV and BV gene families in the sorted CD4+ and CD8+ T cells by GeneScan, demonstrated a standard Gaussian distribution with >8 peaks. CDR3 in CD4+ and CD8+ T cells demonstrated different expression patterns. The majority of CDR3 recombined in frame and the results revealed that there were 10 and 14 amino acid discrepancies between the longest and shortest CDR3 lengths in specific TCR AV and TCR BV gene families, respectively. The results demonstrated that CDR3 polymorphism and length diversity demonstrated different expression and utilization patterns in CD4+ and CD8+ T cells. These results may facilitate future research investigating the porcine TCR CDR3 gene repertoire as well as the functional complexity and specificity of the TCR molecule.

Correspondence to: Dr Zhi-Zhong Jing, State Key Laboratory of Veterinary Etiological Biology, Key Laboratory of Veterinary Public Health of Ministry of Agriculture, Lanzhou Veterinary Research Institute, Chinese Academy of Agricultural Sciences, 1 Xujiaping, Lanzhou, Gansu 730046, P.R. China
E-mail: zhizhongj@163.com

Key words: T cell receptor, immunoscope spectratyping technique, complementarity determining region 3, T cell receptor α chain, T cell receptor β chain

Introduction

Thymus-derived T lymphocytes are involved in adaptive immunity. According to the heterodimer isoform structure of the T cell receptor (TCR) expressed on the surface of T cells, it is possible to divide T lymphocytes into two subsets; αβ and γδ T cells. αβ T cells express TCR α and β chains whereas γδ T cells express TCR γ and δ chains (1,2). The genes encoding TCR α and γ chains [T cell receptor α-locus (*TRA*) and *TRG*, respectively) are composed of a variable region (V), a joining region (J) and a constant region (C). TCR β and δ chains are encoded by *TRB* and *TRD* genes, respectively, which possess additional diversity regions (D) (3,4). Thus, the TCR β chain is more diverse than that of the α chain. A total of 3 hypervariable regions, namely complementarity determining region (CDR) 1, CDR2 and CDR3, have been defined, and collectively form the antigen binding sites. CDR1 and CDR2 are encoded by the V region in germ-line DNA segments, and primarily interact with major histocompatibility complex (MHC) molecules. The CDR3 loop of the TCR α chain is encoded by the terminal of the V region, the foreside of the J region (CDR3 loop of the TCR β chain has an additional D region), and the inserted and deleted sequences during the recombination process, providing significant diversity, which is responsible for the recognition of and interaction with various antigen peptides presented by MHC molecules. As the sequence and length of CDR3 differs according to the type of T cell clone, the sequence of CDR3 determines the structure and specificity of the TCR, where one type of CDR3 sequence represents a specific T cell clonotype (5,6). When a specific TCR recognizes a particular antigen, reactive recombination occurs, which generates a preferential TCR family with the antigen-specific TCR. CDR3 recognizes and binds to a specific antigen, which leads to the clonal expansion of T cells. These antigen-specific T cell clones fulfill a unique immune function (7). Previous studies have revealed that antigen-specific T cells undergo clonal expansion. A Vβ22 monoclonal expansion with an identical CDR3 sequence was detected in the

spleen of patients with type 1 diabetes, and the same Vβ22 TCR was identified in peripheral blood mononuclear cells (PBMCs) (8). The brain-infiltrating T lymphocytes in mice infected with West Nile virus dominantly expressed Vα1-1, Vα2-1, Vβ5-2 and Vβ8-2, which exhibited oligoclonal expansions (9).

The immunoscope spectratyping technique has been proven to be a simple, useful and visual method for detecting polyclonal and oligoclonal expansion of T cells, by determining the CDR3 repertoire in various infectious diseases, including human immunodeficiency virus, viral hepatitis and Epstein-Barr virus (10-12), tumors, including leukemia, colon cancer and melanoma (13,14), transplantation, such as kidney and bone marrow transplantation (15,16), and autoimmune diseases, including systemic lupus erythematosus and rheumatoid arthritis (7,17). The main principle of this technique is to design specific forward TCR α variable region (AV), β variable region (BV) primers, and fluorescence-labeled reverse TCR α chain (AC) and β chain (BC) primers. Following amplification and scanning of the fluorescent polymerase chain reaction (PCR) products, it is possible to acquire the composition and expression frequency of each gene family.

Miniature pigs have been selected as one of the model animals used for medical research into allogeneic immune reactions that occur during organ transplantation (18), due to the advantages of stable heredity, microorganism control and feeding and management (19). Furthermore, porcine immunological studies provide the foundation for the control and prevention of pig diseases. At present, although the molecular structure of porcine TCR at the genomic and transcriptomic levels has been elucidated (20-24), there is limited knowledge of porcine TCR function. Therefore, further investigation of the structure and function of swine TCR is necessary. Furthermore, cluster of differentiation (CD) 4+ and CD8+ T cells generate functional TCRs that recognize peptide-MHC complexes, with CD4+ T cells responding to MHC-class II and CD8+ T cells to MHC-class I; however, it is unclear whether the CDR3 spectratype and sequence length of these T cell subsets are distinct. Previous research has demonstrated that the CDR3 expression frequency and length repertoire of the TCR AV and BV gene families demonstrate specific utilization patterns in PBMCs from healthy pigs and those pigs infected with the classical swine fever virus (CSFV; Fang *et al*, unpublished data). However, the expression frequency and CDR3 length repertoire in individual CD4+ and CD8+ T cell populations remains unknown. In the present study, the CDR3 spectratype of TCR α and β chains was investigated in the two T cell subsets using the immunoscope spectratyping analysis technique. The results of the present study may provide a basis for further study of the functional complexity and specificity of the porcine TCR molecule.

Materials and methods

Animal selection. A total of 3 female healthy Hezuo miniature pigs (age, 10 weeks) originating from the same litter, raised *in situ* at the State Key Laboratory of Veterinary Etiological Biology (Lanzhou, China) were included in the present study. The weight of the animals ranged between 12 and 15 kg. Animals were housed separately, with free access to food and water, and kept on a 12 h light/dark cycle at a temperature of 22˚C, 0.1% CO_2 (v/v) and a humidity of 60%. All pigs were serologically negative for CSFV (cat. no. AP0000297), porcine reproductive and respiratory syndrome (cat. no. KQ0007), the porcine circovirus (cat. no. K703213), the porcine pseudorabies virus (cat. no. AP0000296), the porcine parvovirus (cat. no. K703214) and the foot and mouth disease virus (cat. no AP0001490), as determined using a serological detection kit (Wuhan Keqian Animal Biological Products Co., Ltd., Wuhan, China). All animals were sacrificed in accordance with a protocol approved by the Chinese Ministry of Public Health Guide for the Care and Use of Laboratory Animals (25,26). All animals were euthanized on predetermined days by intramuscular administration of ketamine-xylazine (LGC Science Shanghai, Ltd., Shanghai, China) sedative followed by intravenous administration of 5% sodium pentobarbital solution (100 mg/kg). The present study was approved by the Animal Ethics Committee of Lanzhou Veterinary Research Institute, Chinese Academy of Agricultural Sciences (Lanzhou, China; no. LVRIAEC2015-006).

Isolation of PBMCs. Peripheral blood (15 ml) was obtained from the precaval vein of the healthy miniature pigs, heparinized, and PBMCs were separated by horizontal gradient centrifugation at 400 x g and 20˚C for 20 min using lymphocyte separation medium (Sigma-Aldrich; Merck KGaA, Darmstadt, Germany).

Sorting of CD4+ and CD8+ T cells using magnetic beads. The T cells were first enriched by nylon wool purification (27). This was followed by indirect immunomagnetic positive sorting of CD4+ and CD8+ T cells using a specific combination of magnetic beads (Miltenyi Biotec GmbH, Bergisch Gladbach, Germany) labeled with phycoerythrin-conjugated CD4+ and CD8+ monoclonal antibodies (cat. nos. 559586 and 559584, respectively; BD Biosciences, Franklin Lakes, NJ, USA). T cells were incubated with 1:2 diluted phycoerythrin-conjugated CD4+ and CD8+ monoclonal antibodies for 20 min at 4˚C in the dark, buffer [0.5% bovine serum albumin (BD Biosciences) and 2 mM EDTA in PBS, pH 7.2] was used to wash the cells twice prior to incubation with the microbeads. After 15 min incubation in the dark with the microbeads at 4˚C, the cells were washed with the buffer and centrifuged at 300 x g for 10 min at 4˚C. Cells ($1x10^8$) were loaded onto a MiniMACS Column (Miltenyi Biotec GmbH), and CD4+ and CD8+ T cells were separated according to the manufacturer's protocol. To determine the purity of the separated cells, cells were subsequently centrifuged at 300 x g for 5 min at 4˚C and washed twice with RPMI-1640 medium (Gibco; Thermo Fisher Scientific, Inc., Waltham, MA, USA). Following counting, $1x10^6$ cells were resuspended in 100 μl FACS buffer [2% fetal calf serum (Gibco; Thermo Fisher Scientific, Inc.) and 0.1% sodium azide in PBS], and incubated with fluorescein isothiocyanate-conjugated anti-CD3 antibody (1:100; cat. no. 559582; BD Biosciences, Franklin Lakes, NJ, USA) for 30 min at 4˚C, the cells were washed twice with cold FACS buffer and fixed in PBS containing 2% formaldehyde for 30 min at room temperature prior to flow cytometry analysis with a FACS Calibur flow cytometer (BD Biosciences), and

the results were analyzed using BD CellQuest software (BD Biosciences).

Extraction of RNA and synthesis of cDNA. Total RNA was extracted from the sorted T cell subsets using TRIzol reagent (Invitrogen; Thermo Fisher Scientific, Inc.) according to the manufacturer's protocol. RNA quality was determined by separating total RNA by 1% agarose gel electrophoresis, followed by staining with 10 μg/ml ethidium bromide. Total RNA concentrations were determined using a NanoDrop 2000 Spectrophotometer (Thermo Fisher Scientific, Inc.) and the 260/280 optical density ratio of the RNA was between 1.8 and 2.0. RQ1 RNase-Free DNase (Promega Corporation, Madison, WI, USA) was used to degrade double-stranded and single-stranded DNA according to the manufacturer's instructions.

First strand synthesis of cDNA was performed using the PrimeScript™ 1st strand cDNA Synthesis kit (Takara Biotechnology Co., Ltd., Dalian, China) in a 20 μl reaction mixture according to the manufacturer's protocol. A total of 1 μg RNA was combined with 0.5 μl oligo-dT primer (50 μM), 0.5 μl random hexamers (50 μM), 1 μl dNTP mixture (10 mM) and an appropriate volume of RNase free water (up to 10 μl), mixed gently, heated to 65˚C for 5 min, then immediately chilled on ice. This mixture was then mixed with a reverse transcription (RT) mixture containing 4 μl PrimeScript Buffer (5X), 0.5 μl RNase inhibitor (40 U/μl), 1 μl PrimeScript RTase (200 U/μl) and 4.5 μl RNase free water. The reaction mixture was incubated at 30˚C for 10 min, 42˚C for 50 min and 95˚C for 5 min to inactivate the RTase. The samples were subsequently stored at -80˚C for downstream PCR amplification of TCR gene families.

Normalization of TCR AC and BC-specific cDNA concentrations. The TCR BC-specific cDNA concentration was normalized by amplifying a specific segment of the gene encoding the C region of TCR BC by PCR. Briefly, forward and reverse BC primers (Table I), specific to TCR BC1 and TCR BC2 genes, and Ex Taq DNA polymerase (Takara Biotechnology Co., Ltd.) were used to amplify the specific segment with serial twofold dilutions of cDNA (1:1, 1:2, 1:4, 1:8 and 1:16). Following an initial denaturation step at 95˚C for 5 min, PCR was performed with 30 cycles of denaturation at 94˚C for 50 sec, annealing at 60˚C for 15 sec and extension at 72˚C for 30 sec, with a final extension step at 72˚C for 5 min. The PCR products were then electrophoresed on a 1.5% agarose gel, stained with 10 μg/ml ethidium bromide and photographed using an AlphaImager HP gel imaging system (ProteinSimple, San Jose, CA, USA). The TCR BC specific segment was then quantified using Quantity One 1-D software (version, 4.6.9; Bio-Rad Laboratories, Inc., Hercules, CA, USA). Based on the scanned data, equal quantities of TCR β chain cDNA were estimated and used in the subsequent TCR BV PCR amplification. The TCR AC-specific cDNA concentration was normalized using the same aforementioned methods and specific AC forward and reverse primers were used to amply a specific segment of TCR AC (Table I).

Primers. The primers used for the specific amplification of 19 TCR AV families and 20 TCR BV families were synthesized according to previous studies (28), and are listed in Table I.

PCR amplification of TCR AV and BV families. PCR amplification of TCR AV CDR3 was conducted in a total volume of 25 μl, containing 2 μl first strand cDNA, 0.4 μl 5'-AV primer (100 μM), 0.4 μl carboxyfluorescein (FAM) -labeled reverse AC primer (100 μM), 2.5 μl Taq PCR buffer (10X), 2 μl dNTP mixture (2.5 mM), 0.25 μl Taq DNA polymerase (Takara Biotechnology Co., Ltd.) and 17.45 μl diethylpyrocarbonate (DEPC) water. Primers are listed in Table I. Following an initial denaturation step at 95˚C for 5 min, PCR was conducted with 35 cycles of denaturation at 94˚C for 50 sec, annealing at 60˚C for 15 sec and extension at 72˚C for 30 sec, with a final extension step at 72˚C for 5 min. An aliquot of 8 μl of each PCR product was electrophoresed on a 1.5% agarose gel, stained with 10 μg/ml ethidium bromide and analyzed using an AlphaImager HP gel imaging system (ProteinSimple) and AlphaView software (version, 3.0; ProteinSimple). PCR amplification of TCR BV CDR3 was performed using the identical procedure, except for the use of 5'-BV primer and FAM-labeled reverse BC primers in the PCR reaction mixture (Table I).

GeneScan analysis of the CDR3 spectratype. An aliquot of 2 μl fluorescent PCR product was mixed with 2 μl formamide, 0.5 μl loading dye (25 mM ethylene diamine tetraacetic acid and 50 ng/ml blue dextran) and 0.5 μl GeneScan-500 TAMRA dye-labeled size standards (Applied Biosystems; Thermo Fisher Scientific, Inc.). The mixture was denatured at 95˚C for 2 min, and 2 μl was loaded onto a 6% acrylamide sequencing gel and run for 2 h in a 50-lane Applied Biosystems 373A DNA Sequencer (Applied Biosystems; Thermo Fisher Scientific, Inc.). The data were analyzed using GeneMapper software (version, 4.1; Applied Biosystems; Thermo Fisher Scientific, Inc.).

Sequencing CDR3 in TCR AV and BV families. The PCR amplification mixtures of the TCR gene families with in-frame and out-of-frame CDR3 lengths were amplified in a final volume of 50 μl, containing 4 μl first-stand cDNA, 0.8 μl forward AV or BV primer (100 μM), 0.8 μl unlabeled reverse AC or BC primer (100 μM), 5 μl Taq PCR buffer (10X), 4 μl dNTP mixture (2.5 mM), 0.5 μl Taq DNA polymerase (Takara Biotechnology Co., Ltd.) and 34.9 μl DEPC water. Primer sequences are listed in Table I. The thermal cycling parameters used were the same as those described for the PCR amplification of TCR AV and BV gene families. The PCR products were electrophoresed on a 1.5% agarose gel, stained with 10 μg/ml ethidium bromide, and analyzed under ultraviolet light. They were then purified using a gel extraction kit (Axygen; Corning Incorporated, Corning, NY, USA). The purified PCR products were ligated into the pGEM-T easy vector (Promega Corporation) under the conditions of a 16˚C water-bath overnight according to the manufacturer's protocol. Ligation products (10 ng/μl; 5 μl) were gently added to 50 μl ($5x10^7$ cells) competent DH5α *Escherichia coli* (Takara Biotechnology Co., Ltd.) and were chilled on ice for 30 min, incubated at 42˚C for 90 sec and chilled on ice for 3 min. SOC medium (800 μl; Takara Biotechnology Co., Ltd.) was added to the competent cells and cells were cultured at 37˚C in a constant temperature incubator with a speed of 150 rpm/min for 50 min. The bacterium solution was

centrifuged at 2,500 x g for 5 min at room temperature, 900 µl supernatant was discarded and the bacteria were resuspended using the rest of medium, added evenly to the LB plate (10 g/l tryptone; 5 g/l yeast extract; 10 g/l NaCl; 15 g/l agar power; all from Beijing Solarbio Science &Technology Co., Ltd., Beijing, China) containing 100 µg/ml ampicillin (Sigma-Aldrich; Merck KGaA) and cultured at 37˚C for 15 h. Positive clones were selected using ampicillin and nucleotide sequences were determined by Genescript Co., Ltd (Nanjing, China).

Statistical analysis. The average fluorescence intensity of each gene family in the T cell subsets was calculated, and the nonparametric two-tailed Mann-Whitney-Wilcoxon rank sum test was used for the comparison of independent variables using SPSS software (version, 18.0; SPSS, Inc., Chicago, IL, USA). $P<0.05$ was considered to indicate a statistically significant difference.

Results

RT-PCR amplifications of TCR AV and TCR BV gene families in CD4+ and CD8+ T cells. RT-PCR products of 19 TCR AV families (including one subfamily, AV8-4S) and 20 TCR BV families (including one subfamily, BV12A) in sorted CD4+ and CD8+ T cells were separated by 1.5% agarose gel electrophoresis and stained with 10 µg/ml ethidium bromide (Fig. 1A and B). The majority of gene families demonstrated clear, specific and expected ~250 bp fragment sizes when separated by 1.5% agarose gel electrophoresis (Fig. 1A and B), which indicated that detection of the expression of specific TCR AV and TCR BV families is possible. Compared with other PCR products, the PCR products of the TCR AV39 gene family presented an obscure band (lower intensity), of the expected size, indicating that AV39 may adopt a relatively low level of expression compared with other TCR gene families. In total, ~8 bands differing in length by 3 bp were observed for each TCR AV or BV gene family in the sequencing gels (Fig. 1C and D).

GeneScan analysis of the CDR3 spectratype of TCR Vα and Vβ chains. The results were analyzed using GeneMapper 4.1 software, which transforms the size, type and quantity of different fragments into a visual waveform graph. The length repertoire and diversity of CDR3 in 19 TCR AV families and 20 TCR BV families is shown in Fig. 2A. The peak map of CDR3 length of all the TCR AV and BV gene families demonstrated a Gaussian distribution, indicating polyclonal T cell proliferation. At least eight peaks with different DNA fragment sizes and fluorescence intensities were observed in each family (Fig. 1). TCR BV11S demonstrated a dual Gaussian distribution pattern profile in CD4+ and CD8+ T cell subpopulations, which is in accordance with results observed in PBMCs in previous studies (19,28). Two TCR AV gene families (AV3S and AV8-3S) and 2 TCR BV gene families (BV2S and BV3S) were selected at random in the present study to clearly demonstrate the Gaussian distribution of CDR3 spectratypes and 3 bp sequence discrepancy between two adjacent peaks (Fig. 2B).

Length analysis of the CDR3 sequence. The sequence length of the CDR3 region was then examined, and the majority of CDR3 in the TCR AV and TCR BV families of CD4+ and CD8+ T cell subsets were revealed to be recombined in frame, with a 3-bp gap between two adjacent CDR3 products (Tables II and III). However, specific CDR3 sequences were identified to be out-of-frame, demonstrating 1-2 or ≥4 bp unconformity. This same discrepancy between adjacent CDR3 sequences was observed in the CD4+ and CD8+ T cell subsets. In addition, CDR3 length discrepancy between the shortest and the longest sequences in all families were between 15 and 42 bp, with the largest 30 bp gap (10 amino acids) in TCR AV observed in CD4+ T cells and 27 bp (9 amino acids) in CD8+ T cells (Table II). The largest 33 bp discrepancy (11 amino acids) between the shortest and the longest CDR3 sequence within the same gene family in TCR BV was observed in CD4+ T cells, and 42 bp (14 amino acids) in CD8+ T cells (Table III).

Following sequencing of CDR3 in the TCR gene families with in-frame and out-of-frame CDR3 lengths, the out-of-frame CDR3 sequence was revealed to be present in TCR AV and BV gene families of CD4+ and CD8+ T cells.

Expression frequency of CDR3. The average fluorescence intensity of each TCR AV and BV gene family was then determined. The results demonstrated that the expression frequencies of CDR3 in gene families of the same subset were different, as was the CDR3 expression frequency in same gene family between CD4+ and CD8+ T cell subpopulations (Fig. 3A and B). The CD4+/CD8+ mean fluorescence intensity ratio among the different gene families is shown in Fig. 3C. A significantly higher mean fluorescence intensity of AV26 ($P=0.039$) and BV30 ($P=0.01$), and a significantly lower mean fluorescence intensity of BV24 ($P=0.007$) was observed in the CD4+ population when compared with the CD8+ population (Fig. 3C). The majority of the CD4+/CD8+ ratios in the TCR AV gene families were <1.2, except for AV2S, AV26, AV38 and AVX. In addition, the ratios in 11 TCR BV gene families (BV6S, BV9S, BV11S, BV12S, BV12AS, BV15S, BV19S, BV21, BV27, BV30 and BVXS) were >1.2 (Fig. 3C). The ratios were close to 1 in the TCR AV5S, AV13S, AV14, AV21S and AV39 gene families, as well as the TCR BV3S, BV4S, BV10S, BV19S and BV25 gene families, indicating similar fluorescence intensity values of CDR3 in these families in CD4+ and CD8+ T cells.

Discussion

The present study elucidated the patterns and length distributions of the CDR3 repertoire of TCR AV and BV gene families in separated CD4+ and CD8+ T cell populations from miniature pigs using the immunoscope spectratyping technique. In addition, the expression frequencies of CDR3 in the sorted T cells were compared. The CD4+ and CD8+ T cell populations demonstrated specific expression of all TCR AV and BV gene families, and a typical Gaussian distribution model was observed for each gene family. The majority of CDR3 was observed to recombine in-frame, and the expression frequency of CDR3 in the same family was different between CD4+ and CD8+ T cell populations. The results of the present study revealed the abundant diversity of CDR3 in CD4+ and CD8+ T cells.

The CDR3 PCR products of the 19 TCR AV and 20 TCR BV gene families exhibited a clear, specific band of the

Table I. Primer sequences used for TCR AV/BV-specific amplifications.

A, TCR AV family

Variable region	Primer sequence (5'-3')	Expected size (bp)
DV1	TGGCTGGAATGCAAAGGAAGA	220
AV2S	TCAGGTGCAGGTGGCAGATG	150
AV3S	CCAGCTGTCCTAGGGAGCGACT	150
AV4S	GGCCACCCTGAAAGACACTGC	210
AV5S	AAAATCACAGCAGCCCAACCTG	153
AV6S	GAGCACCACCTTTGACACCAGAG	200
AV8-3S	TCCAGTACCCCAGCCAAGGA	280
AV8-4S	CAGAGGCTTTGGGGCTGAAT	270
AV12S	GCAAGCATGTCTCCCTGCTCA	170
AV13S	CTCCCTGCACATCGCAGTCA	170
AV14	TCTCAGATGCACAGGTGGAGGA	160
AV16S	CCTCGACAAGAAAGAGGCATCC	200
AV18S	TCTTCCAGAGGAGGCACCTATGAC	350
AV21S	CGAGAGGGAGACGGCTTGGT	340
AV22	GGCGGCCTCATCAATCTGTTT	250
AV25S	GGACAGCTCCCTGCACATCA	160
AV26	TCGGCAAAATCCCAATCAGA	280
AV38	AGCTTCCCAACGGGGAGATG	270
AV39	ACCAAAGCCCATTGCAGCAC	180
AVX	TCGACAGTATCCAAATCAGGCACT	280
AC-FAM	TTTGGGGCCTTTCAGCTGGT	
AC forward	CTGTGATGCCAAGTTGGTAG	135
AC reverse	CACAGCCGCAGTGTCATGAG	

B, TCR BV family

Variable region	Primer sequence (5'-3')	Expected size (bp)
BV2S	GGCACGTACCTGACTCTGAA	190
BV3S	ACAGTTCCACGTCGCTTCTT	220
BV4S	CAGATACCTGGTCCTGGGAA	370
BV5S	CACCGAGACATCTGATTAAAGC	380
BV6S	TGGCATCACTGACAAAGGAG	250
BV7S	TCTGAGCTGAAATTGCTCTCC	190
BV9S	AGCTTTTGTCTCCACAGGTCA	400
BV10S	CCTGTGATGTTGGCATCCTT	260
BV11S	TGTTTCTCAGTTGCCCCAGA	210
BV12S	CACCCAGACACGAGGTGA	340
BV12A	CAACAACGGGTCTCCTGTG	230
BV15S	CGGCCTAACCCTTCTTTCTG	210
BV19S	CATTGACGCAGAAGAACCAG	200
BV20	ACAGCGCCAAGTTTCTCATC	230
BV21	ACAGCGATTTACAGCCGAGT	210
BV24[a]	CTTTGTGGCCTTTTGCATCC	420
BV25	CACCAGCCCTTCACAGACAT	180
BV27	AGCCGAATTTCCCCTTGAT	190
BV29	ACCGTCAGCTTCTAGGACAAAG	390
BV30	TGACCAGAAAGATCCTGAAAAG	400
BVXS	ATCCCTTCCTGGAGCAGATT	220
BC-FAM	ATCTCCGCTTCCGATGGT	
BC forward	GGACCTGCAGCAGGTGAGAC	110
BC reverse	GTAGAAGCCTGTGGCCAGGC	

[a]Primer sequence is different to those used in the references provided in the materials and methods section. TCR, T cell receptor; AV, α variable region; BV, β variable region; AC, α chain, BC, β chain; FAM, carboxyfluorescein.

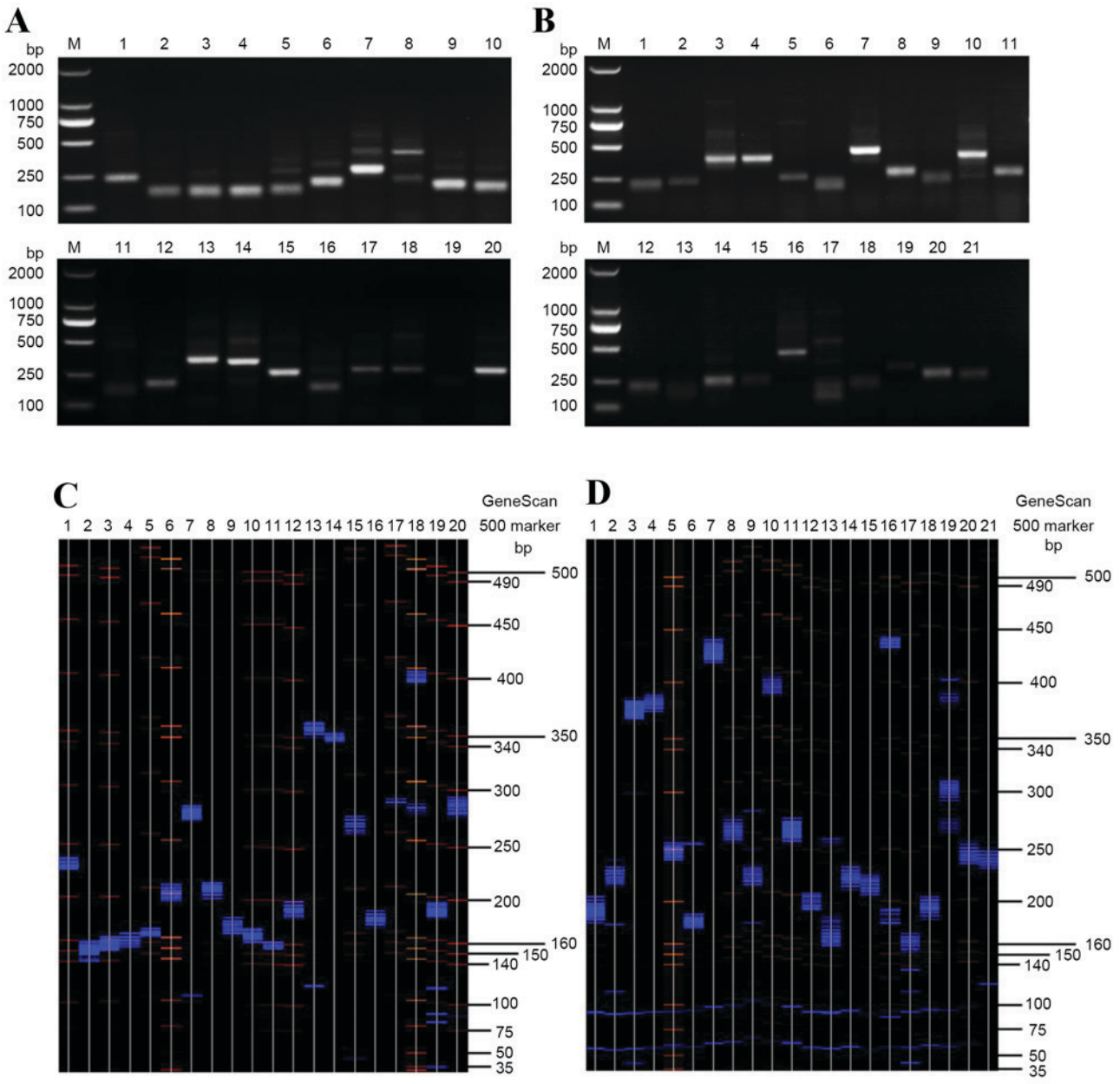

Figure 1. The distribution profile of complementarity determining region 3 length in 19 TCR AV families and 20 TCR BV families from healthy miniature pigs. (A) RT-PCR products of 19 TCR AV gene families in separated CD4+ T cells. Lane M represents the DNA ladder, and lanes 1-20 represent the following TCR AV families: DV1, AV2S, AV3S, AV4S, AV5S, AV6S, AV8-3S, AV8-4S, AV12S, AV13S, AV14, AV16S, AV18S, AV21S, AV22, AV25S, AV26, AV38, AV39 and AVX, respectively. (B) RT-PCR products of 20 TCR BV gene families in separated CD4+ T cells. Lane M represents the DNA ladder and lanes 1-21 represent the following TCR BV families: BV2S, BV3S, BV4S, BV5S, BV6S, BV7S, BV9S, BV10S, BV11S, BV12S, BV12A, BV15S, BV19S, BV20, BV21, BV24, BV25, BV27, BV29, BV30 and BVXS, respectively. (C) Numbers 1-20 denote the corresponding RT-PCR products of TCR AV families from DV1 to AVX, separated on a 6% acrylamide sequencing gel. (D) Numbers 1-21 denote the corresponding RT-PCR products of TCR BV families from BV2S to BVXS, separated on a 6% acrylamide sequencing gel. The blue bands represent the PCR products of the TCR gene families. TCR AV, T cell receptor α variable region; TCR BV, T cell receptor β variable region; CD, cluster of differentiation; RT-PCR, reverse transcription-polymerase chain reaction.

expected size on the 1.5% agarose gel electrophoretogram, suggesting that the TCR gene families demonstrated specific expression patterns in the T cell subsets. In the sequencing gel, >8 bands with a 3-bp gap were observed in the majority of the gene families.

Theoretically, spectratypes of the CDR3 region demonstrate a Gaussian distribution in immune homeostasis (27). In the present study, the majority of CDR3 length distributions followed this pattern, and >8 peaks in each gene family were observed. However, in CD4+ and CD8+ T cells, TCR BV11S exhibited a dual Gaussian distribution profile, which was consistent with the results of previous studies involving PBMCs from healthy pigs (19,28).

In the present study, the detailed size of CDR3 sequences in various families was investigated, and >8 different sequence lengths in each family were observed, implying the polyclonal proliferation of TCR αβ T cells in normal pigs. According to clonal selection theory, abortion rearrangement is conceivable during VDJ recombination, and P/N insertion (29) increases this probability (19). However, all CDR3 genes in mature

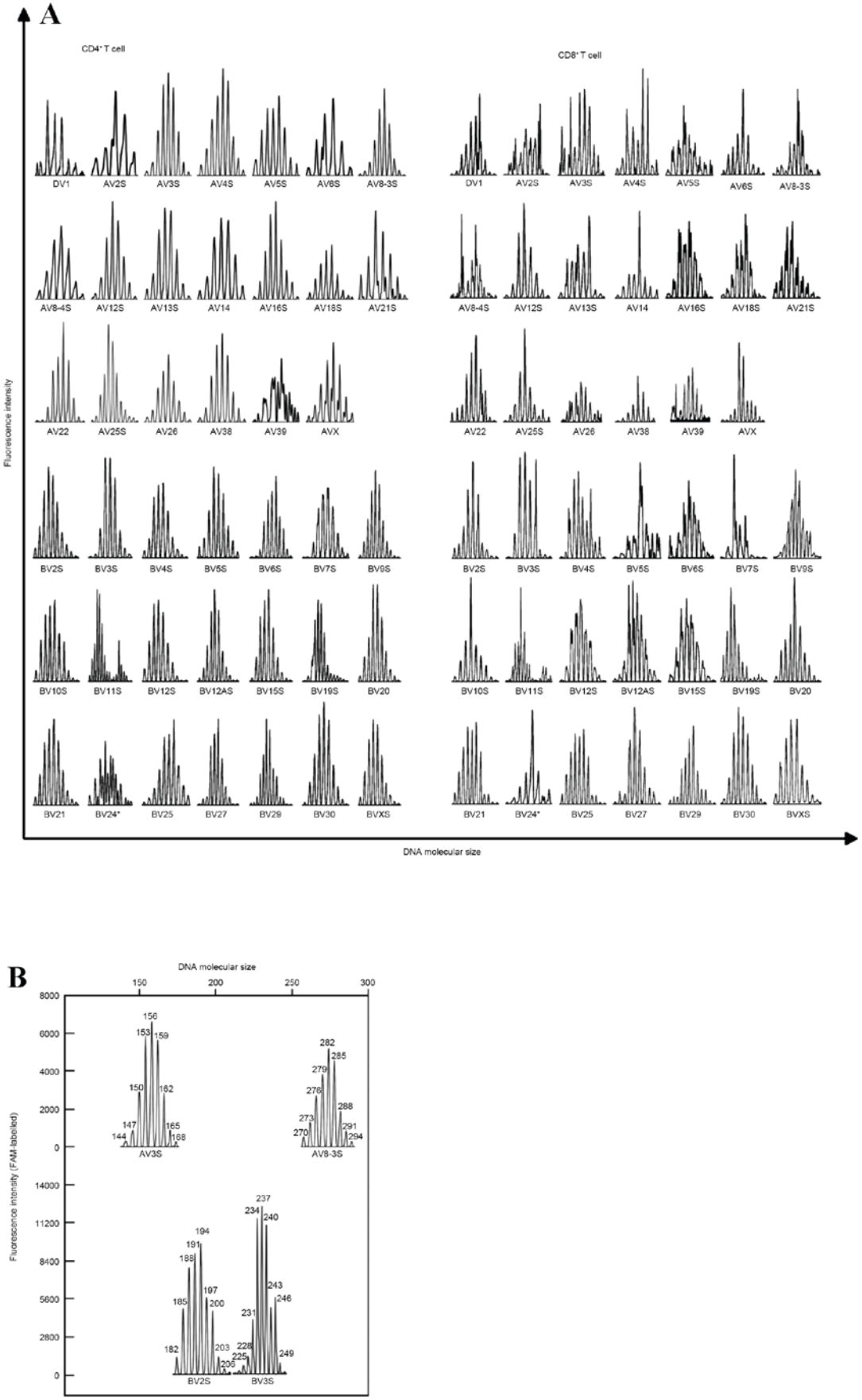

Figure 2. CDR3 spectratypes in healthy miniature pigs. (A) CDR3 spectratypes of 19 TCR AV and 20 TCR BV families from CD4+ and CD8+ T cells were analyzed. The x-axis of each plot corresponds to the molecular size of the DNA, and the relative fluorescence intensity of the peaks is plotted on the y-axis. (B) CDR3 fragment size and fluorescence intensity analysis of TCR AV3S, AV8-3S, BV2S and BV3S in CD4+ T cells. Results are representative of results in CD4+ and CD8+ T cells. CDR3, complementarity determining region 3; TCR AV, T cell receptor α variable region; TCR BV, T cell receptor β variable region; CD, cluster of differentiation; FAM, carboxyfluorescein.

Table II. GeneScan analysis of CDR3 length in $CD4^+$ and $CD8^+$ T cells of TCR AV families.

A, $CD4^+$ T cells, bp

DV 1	AV 2S	AV 3S	AV 4S	AV 5S	AV 6S	AV 8-3S	AV 8-4S	AV 12S	AV 13S	AV 14S	AV 16S	AV 18S	AV 21	AV 22	AV 25	AV 26	AV 38	AV 39	AV XS
223	141	144	138	135	194	270	203	171	158	149	182	345	337	252	158	264	267	184	272
226	144	147	141	138	197	273	206	174	161	152	185	348	340	255	161	267	270	***185***	275
229	147	150	144	***142***	200	276	209	177	164	155	188	351	343	258	164	270	273	***186***	278
232	***151***	153	***148***	145	203	279	212	180	167	158	191	354	346	***260***	167	273	276	187	281
235	154	156	151	148	206	282	215	183	170	161	194	***356***	349	263	170	276	279	***188***	284
238	157	159	154	151	209	***284***	218	186	173	164	197	359	352	266	173	279	282	***189***	287
241	160	162	157	154	212	287	221	189	176	167	200	362		269	176	282	***284***	190	***289***
244	163	165	160	157	215	290	224			170	203	365			179	***284***	287	***194***	292
		168	163	160											182	287			295
				163											185				
				166											188				
				169															

B, $CD8^+$ T cells, bp

DV 1	AV 2S	AV 3S	AV 4S	AV 5S	AV 6S	AV 8-3S	AV 8-4S	AV 12S	AV 13S	AV 14S	AV 16S	AV 18S	AV 21	AV 22	AV 25	AV 26	AV 38	AV 39	AV XS
225	144	140	138	153	194	266	198	168	158	149	182	339	337	246	164	268	267	192	275
228	147	143	141	156	197	269	201	171	161	152	185	342	340	249	167	271	270	195	278
231	150	***147***	144	159	200	272	204	174	164	155	188	345	343	252	170	274	273	198	281
234	153	150	***148***	***160***	203	275	207	177	167	158	191	348	346	255	173	***276***	276	201	284
237	***154***	153	151	163	206	278	210	180	170	161	194	351	349	258	176	279	279	204	287
240	157	156	154	166	209	281	***211***	183	173	164	197	354	352	***260***	179	282	282	207	***289***
	160	159	157	169		284	214	186	176	167	200	357	355	263	182	285	285		292
		162	160	172		287	217	189	179	170	203	360	358	266		288			295
		165	163			290					206	363		269					
												366							

The majority of CDR3 sequences in the TCR AV families recombined in-frame. However, out-of-frame gene rearrangements were additionally observed. Particular families demonstrated a 1-2 bp discrepancy (the numbers representing CDR3 sequence length were indicated with italic, underline and bold) and others exhibited ≥4 bp discrepancy (indicated with italic and bold). CDR3, complementarity determining region 3; TCR AV, T cell receptor α variable region.

Table III. GeneScan analysis of CDR3 length in the $CD4^+$ and $CD8^+$ T cells of TCR BV families.

A, $CD4^+$ T cells, bp

BV2S	BV3S	BV4S	BV5S	BV6S	BV7S	BV9S	BV10S	BV11S	BV12S	BV12AS	BV15S	BV19S	BV20	BV21	BV24	BV25	BV27	BV29	BV30	BVXS
182	215	369	372	238	176	415	248	199	376	248	190	157	211	207	430	150	181	291	235	217
185	218	372	375	241	179	418	251	202	379	251	193	160	214	210	433	153	184	294	238	220
188	221	***376***	378	244	***181***	421	254	205	***381***	254	196	163	217	***214***	436	156	187	297	241	223
191	224	380	381	247	184	424	257	208	384	257	199	166	220	217	***438***	159	190	300	244	226
194	227	383	***383***	250	187	427	260	211	387	***259***	202	169	223	220	441	162	193	303	247	229
196	***231***	386	386	253	190	430	***262***	214	390	262	205	172	226	223	***445***	165	196	306	250	232
199	234	389	389	256	193	433	265	217	393	265	***209***	175	***230***	226	448	168	199	309	253	235
202	237	392	392	259	196	436	268	***224***	396	268	212	178	233	229	451	171	202	312	256	238
	240	395	395			439	271	227		271	215	181	236	232	***455***	174		315		241
						442		***233***				184	239	235	458					
								236				187			461					
								239				190			464					
								242												
								245												

B, CD8+ T-cells, bp

BV2S	BV3S	BV4S	BV5S	BV6S	BV7S	BV9S	BV10S	BV11S	BV12S	BV12AS	BV15S	BV19S	BV20	BV21	BV24	BV25	BV27	BV29	BV30	BVXS
182	225	370	377	241	178	415	248	202	372	248	193	160	211	211	430	153	181	286	232	217
185	228	373	380	244	181	418	251	205	375	251	196	163	214	214	433	156	184	289	235	220
188	231	376	383	***246***	184	421	254	208	378	254	199	166	217	217	436	159	187	292	238	223
190	234	379	386	247	186	424	257	***210***	381	257	202	169	220	220	439	162	190	295	241	226
193	237	382	389	250	189	427	260	211	384	***259***	205	172	223	223	442	165	193	***297***	244	229
197	240	385	392	253		430	***262***	***215***	387	262	208	175	***227***	226	***448***	168	196	300	247	232
200	243	388		256		433	265	217	390	265	211	178	230	229	451	171	199	303	250	265
203		391		259		436	268	220	393	268	214		233	232		174	202	306	253	268
206						439		***235***		271	217		236	235		***179***		309	256	241
209								238						238				312	259	
								241										315		
								244												

The majority of CDR3 sequences in the TCR BV families recombined in-frame. However, out-of-frame gene rearrangement was additionally observed. Particular families demonstrated a 1-2 bp discrepancy (the numbers representing CDR3 sequence length were indicated with italic, underline and bold) and others exhibited ≥4 bp discrepancy (indicated with italic and bold). CDR3, complementarity determining region 3; TCR BV, T cell receptor β variable region.

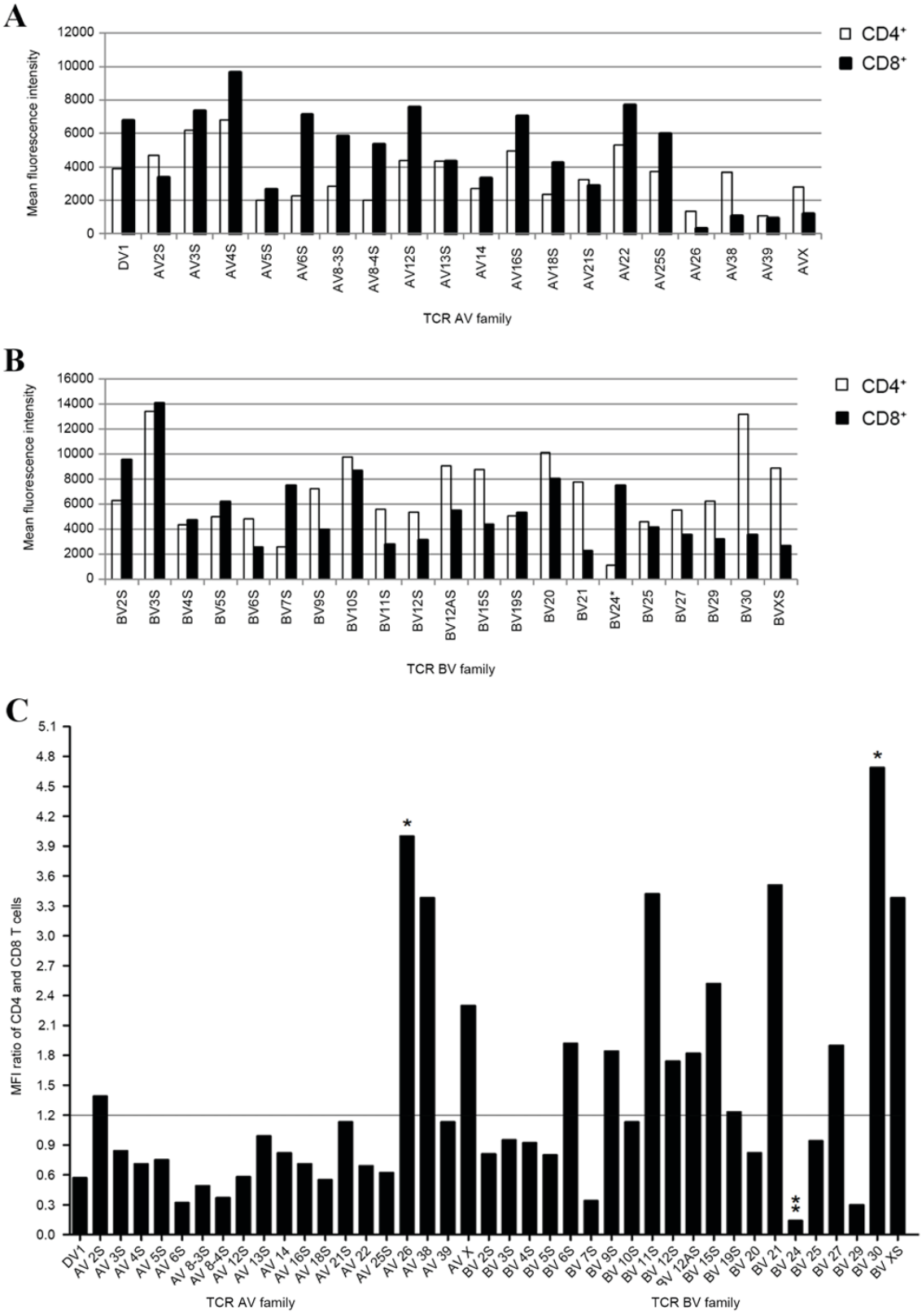

Figure 3. Differential mean fluorescence intensities of CDR3 in TCR AV and TCR BV families in the CD4+ and CD8+ T cells of healthy miniature pigs. (A) The expression frequency of CDR3 in (A) TCR AV and (B) TCR BV gene families in CD4+ and CD8+ T cells. (C) The MFI ratio of CD4+ and CD8+ T cells within the same gene family. *P<0.05 and **P<0.01 vs. CD8+ T-cell subset. CDR3, complementarity determining region 3; TCR AV, T cell receptor α variable region; TCR BV, T cell receptor β variable region; CD, cluster of differentiation; MFI, mean fluorescence intensity.

T cells following positive and negative selection in peripheral blood should be in-frame. The results of the present study demonstrated that the majority of the CDR3 genes were recombined in-frame, with a 3-bp gap between two adjacent CDR3 lengths; whereas the remaining demonstrated 1, 2, 4 or >4-bp discrepancies. Meanwhile, those gene families with

out-of-frame CDR3 lengths were cloned and sequenced, and these out-of-frame CDR3 sequences were revealed to exist in both $CD4^+$ and $CD8^+$ T cells. A previous study investigating CDR3 TCR β chain diversity in porcine PBMCs additionally observed this phenomenon (19). These specific characteristics of CDR3 have been demonstrated in the present study, as well as a number of previous studies (28,30). Specific TCR BV CDR3 lengths between two adjacent CDR3 products in the PBMCs of miniature pigs revealed a 1-bp gap (28). The same 1-2 bp or ≥6 bp discrepancy was observed in four normal volunteers following the analysis of the CDR3 length repertoire and diversity of TCR α chains in human peripheral blood T lymphocytes (30). To the best of our knowledge, there are currently no reports regarding in-frame/out-of-frame rearrangements of CDR3 at the mRNA level in peripheral T cells. These out-of-frame CDR3 features may be derived from individual germ-line gene sequences or belong to the pseudogene family (31). In addition, 10 amino acid residue discrepancies were observed in specific TCR AV gene families between the longest and shortest CDR3 sequence, and 14 amino acid residues in several TCR BV gene families in the present study. A comparison of antigenic peptides in a previous study revealed that the TCR CDR3 segments were more diverse in length, potentially due to the weaker association of antigenic peptides with the TCR than with the MHC (32). Although the CDR3 length repertoire is determined during thymic selection and maintained in the peripheral blood, it differed between $CD4^+$ and $CD8^+$ T cells in the present study. Pannetier *et al* (33) observed that different TCR BV subsets prefer different CDR3 lengths. However, whether there is a clear difference between $CD4^+$ and $CD8^+$ T cells remains to be verified.

Average fluorescence intensity analysis of CDR3 in the present study, revealed that different gene families exhibited variable expression frequencies, and that the same gene family demonstrated different expression frequencies between the two T cell subsets. Mean fluorescence intensity analysis revealed that AV26 and BV30 families displayed significantly higher levels of expression frequency, and BV24 exhibited significantly lower levels of expression frequency in $CD4^+$ T cells when compared with $CD8^+$ T cells. From the overall levels of expression frequency, the majority of TCR AV families in $CD4^+$ T cells demonstrated relatively low expression levels, whereas >50% of the TCR BV gene families were overexpressed when compared with $CD8^+$ T cells. Unlike a previous study involving PBMCs (19), BV9S, BV21 and BV3S families were the most frequently expressed, and the expression frequency of BV24 was low in all experimental animals.

In conclusion, the present study demonstrated the length and expression frequency of the CDR3 repertoire of the TCR AV and TCR BV gene families in separated $CD4^+$ and $CD8^+$ T cells. All detected TCR AV and TCR BV gene families were universally expressed in the two T cell subsets, and presented with a standard Gaussian distribution pattern, except for TRBV11S that exhibited a dual Gaussian distribution profile. Knowledge of the diversity of CDR3 sequence lengths and the nonuniform patterns of expression, may provide a more detailed understanding of porcine TCR gene recombination, and provide an explanation for the high number of CDR3 polymorphisms and TCR CDR3 repertoire drift that occur under a pathogenic status. However, the mechanisms of restrictive use of the TCR gene families and the CDR3 length diversity in the T cell subsets under pathological conditions require further clarification.

Acknowledgements

The present study was supported by the National Natural Science Foundation of China (grant no. 31372423).

References

1. Davis MM, Boniface JJ, Reich Z, Lyons D, Hampl J, Arden B and Chien Y: Ligand recognition by alpha beta T cell receptors. Ann Rev Immunol 16: 523-544, 1998.
2. Davis MM: T cell receptor gene diversity and selection. Ann Rev Biochem 59: 475-496, 1990.
3. Rowen L, Koop BF and Hood L: The complete 685-kilobase DNA sequence of the human betaT cell receptor locus. Science 272: 1755-1762, 1996.
4. Allison TJ, Winter CC, Fournié J-J, Bonneville M and Garboczi DN: Structure of a human gammadelta T-cell antigen receptor. Nature 411: 820-824, 2001.
5. Gorski J, Yassai M, Zhu X, Kissela B, Kissella B [corrected to Kissela B], Keever C and Flomenberg N: Circulating T cell repertoire complexity in normal individuals and bone marrow recipients analyzed by CDR3 size spectratyping. Correlation with immune status. J Immunol 152: 5109-5119, 1994.
6. Höhn H, Neukirch C, Freitag K, Necker A, Hitzler W, Seliger B and Maeurer MJ: Longitudinal analysis of the T-cell receptor (TCR)-VA and-VB repertoire in CD8+ T cells from individuals immunized with recombinant hepatitis B surface antigen. Clin Exp Immunol 129: 309-317, 2002.
7. Luo W, Ma L, Wen Q, Wang N, Zhou MQ and Wang XN: Analysis of the interindividual conservation of T cell receptor alpha- and beta-chain variable regions gene in the peripheral blood of patients with systemic lupus erythematosus. Clin Exp Immunol 154: 316-324, 2008.
8. Codina-Busqueta E, Scholz E, Muñoz-Torres PM, Roura-Mir C, Costa M, Xufré C, Planas R, Vives-Pi M, Jaraquemada D and Martí M: TCR bias of in vivo expanded T cells in pancreatic islets and spleen at the onset in human type 1 diabetes. J Immunol 186: 3787-3797, 2011.
9. Kitaura K, Fujii Y, Hayasaka D, Matsutani T, Shirai K, Nagata N, Lim CK, Suzuki S, Takasaki T, Suzuki R and Kurane I: High clonality of virus-specific T lymphocytes defined by TCR usage in the brains of mice infected with West Nile virus. J Immunol 187: 3919-3930, 2011.
10. González-Serna A, Abad-Fernández M, Soriano-Sarabia N, Leal M and Vallejo A: CD8 TCR β chain repertoire expansions and deletions are related with immunologic markers in HIV-1-infected patients during treatment interruption. J Clin Virol 58: 703-709, 2013.
11. Maru Y, Yokosuka O, Imazeki F, Saisho H and Omata M: Analysis of T cell receptor variable regions and complementarity determining region 3 of infiltrating T lymphocytes in the liver of patients with chronic type B hepatitis. Intervirology 46: 277-288, 2003.
12. Gras S, Wilmann PG, Chen Z, Halim H, Liu YC, Kjer-Nielsen L, Purcell AW, Burrows SR, McCluskey J and Rossjohn J: A structural basis for varied αβ TCR usage against an immunodominant EBV antigen restricted to a HLA-B8 molecule. J Immunol 188: 311-321, 2012.
13. Rezvany M-R, Jeddi-Tehrani M, Wigzell H, Osterborg A and Mellstedt H: Leukemia-associated monoclonal and oligoclonal TCR-BV use in patients with B-cell chronic lymphocytic leukemia. Blood 101: 1063-1070, 2003.
14. Luo W, Liao WJ, Huang YT, Shi M, Zhang Y, Wen Q, Zhou MQ and Ma L: Normalization of T cell receptor repertoire diversity in patients with advanced colorectal cancer who responded to chemotherapy. Cancer Sci 102: 706-712, 2011.
15. Hirokawa M, Matsutani T, Saitoh H, Ichikawa Y, Kawabata Y, Horiuchi T, Kitabayashi A, Yoshioka T, Tsuruta Y, Suzuki R, *et al*: Distinct TCRAV and TCRBV repertoire and CDR3 sequence of T lymphocytes clonally expanded in blood and GVHD lesions after human allogeneic bone marrow transplantation. Bone Marrow Transplant 30: 915-923, 2002.

16. Gorski J, Yassai M, Keever C and Flomenberg N: Analysis of reconstituting T cell receptor repertoires in bone marrow transplant recipients. Arch Immunol Ther Exp (Warsz) 43: 93-97, 1995.
17. Kim G, Tanuma N and Matsumoto Y: Stage-dependent usage of TCR alpha chains with different CDR3 motifs by spinal cord T cells in autoimmune encephalomyelitis. J Neuroimmunol 96: 66-72, 1999.
18. Gianello P, Fishbein JM and Sachs DH: Tolerance to primarily vascularized allografts in miniature swine. Immunol Rev 133: 19-44, 1993.
19. Yao WJ, Fang YX, Jia HJ, He XB, Zeng S, Chen GH, Liu TA and Jing ZZ: Diversity and molecular genetic characteristics of porcine T cell receptor β chain. Vet Sci Chi 44: 641-649, 2014.
20. Yamamoto R, Uenishi H, Hatsuse H, Sato E, Awata T, Yasue H and Takagaki Y: TRAV gene usage in pig T-cell receptor alpha cDNA. Immunogenetics 57: 219-225, 2005.
21. Baron C, Sachs DH and LeGuern C: A particular TCR beta variable region used by T cells infiltrating kidney transplants. J Immunol 166: 2589-2596, 2001.
22. Butler JE, Wertz N, Sun J and Sacco RE: Comparison of the expressed porcine Vbeta and Jbeta repertoire of thymocytes and peripheral T cells. Immunology 114: 184-193, 2005.
23. Watanabe M, Iwasaki Y, Mita Y, Ota S, Yamada S, Shimuzu M and Takagaki Y: Porcine T-cell receptor beta-chain: A genomic sequence covering Dbeta1. 1 to Cbeta2 gene segments and the diversity of cDNA expressed in piglets including novel alternative splicing products. Mol Immunol 44: 2332-2343, 2007.
24. Eguchi-Ogawa T, Toki D and Uenishi H: Genomic structure of the whole D-J-C clusters and the upstream region coding V segments of the TRB locus in pig. Dev Comp Immunol 33: 1111-1119, 2009.
25. Li T, He X, Jia H, Chen G, Zeng S, Fang Y, Jin Q and Jing Z: Molecular cloning and functional characterization of murine toll-like receptor 8. Mol Med Rep 13: 1119-1126, 2016.
26. Chen G, Zeng S, Jia H, He X, Fang Y, Jing Z and Cai X: Adjuvant effect enhancement of porcine interleukin-2 packaged into solid lipid nanoparticles. Res Vet Sci 96: 62-68, 2014.
27. Luo W, Liao WJ, Ma L, Huang YT, Shi M, Wen Q and Wang XN: Dynamic monitoring the TCR CDR3 spectratypes in patients with metastatic CRC treated with a combination of bevacizumab, irinotecan, fluorouracil, and leucovorin. Cancer Immunol Immunother 59: 247-256, 2010.
28. Yao WJ: Dynamic changes of T cell receptor α and β chain variable regions in the peripheral blood mononuclear cells of the infected pigs by C-strain classical swine fever virus (unpublished PhD thesis). Chinese Academy of Agricultural Sciences, 2014.
29. Fazilleau N, Cabaniols JP, Lemaître F, Motta I, Kourilsky P and Kanellopoulos JM: Valpha and Vbeta public repertoires are highly conserved in terminal deoxynucleotidyl transferase-deficient mice. J Immunol 174: 345-355, 2005.
30. Yao XS, Diao Y, Sun WB, Luo JM, Qin M and Tang XY: Analysis of the CDR3 length repertoire and the diversity of TCR alpha chain in human peripheral blood T lymphocytes. Cell Mol Immunol 4: 215-220, 2007.
31. Nemazee D: Receptor editing in lymphocyte development and central tolerance. Nat Rev Immunol 6: 728-740, 2006.
32. Nishio J, Suzuki M, Nanki T, Miyasaka N and Kohsaka H: Development of TCRB CDR3 length repertoire of human T lymphocytes. Int Immunol 16: 423-431, 2004.
33. Pannetier C, Cochet M, Darche S, Casrouge A, Zöller M and Kourilsky P: The sizes of the CDR3 hypervariable regions of the murine T-cell receptor beta chains vary as a function of the recombined germ-line segments. Proc Natl Acad Sci USA 90: 4319-4323, 1993.